Protein Science (1998), 7:1857–1867. Cambridge University Press. Printed in the USA.

Kinetic epitope mapping of the chicken lysozyme·HyHEL-10 Fab complex: Delineation of docking trajectories

MARC G. TAYLOR,[1,4] ARVIND RAJPAL,[2] AND JACK F. KIRSCH[1,2,3]

[1]Center for Advanced Materials, Lawrence Berkeley National Laboratory, Berkeley, California 94720
[2]Department of Chemistry, University of California, Berkeley, California 94720
[3]Department of Molecular and Cell Biology, Division of Biochemistry and Molecular Biology, University of California, Berkeley, California 94720

(RECEIVED February 12, 1998; ACCEPTED June 1, 1998)

Abstract

The rate constants, k_{on}, for the formation of hen (chicken) lysozyme (HEWL)·Fab-10 complexes have been determined for wild-type (WT) and epitope-mutated lysozymes by a homogeneous solution method based on the 95% reduced enzymatic activity of the complex. The values fall within a narrow 10-fold range [(0.18 to 1.92) $\times 10^6$ M^{-1} s^{-1}]. The affinity constants, K_D, cover a broader, 440-fold, range from 0.075 to 33 nM. Values of K_D as high as 7 μM were obtained for the complexes prepared from some mutations at HEWL positions 96 and 97, but the associated kinetic constants could not be determined. The values of k_{on} are negatively correlated with side-chain volume at position 101_{HEWL}, but are essentially independent of this parameter for position 21_{HEWL} substitutions. The multiple mutations made at positions 21_{HEWL} and 101_{HEWL} provide sufficient experimental data on complex formation to evaluate Φ values [$\Phi = (\Delta\Delta G^{\ddagger}_{on})/(\Delta\Delta G_D)$] at these two positions to begin to define trajectories for protein–protein association. The data, when interpreted within the concept of a two-step association sequence embracing a metastable encounter complex intermediate, argue that the rate determining step at position 21_{HEWL} ($\Phi_{avg} = 0.2$) is encounter complex formation, but the larger Φ_{avg} value of 0.36 experienced for most position 101_{HEWL} mutations indicates a larger contribution from the post-encounter annealing process at this site for these replacements.

Keywords: epitope mapping; hen (chicken) egg-white lysozyme; HyHEL-10; monoclonal antibody; protein–protein interaction; site-directed mutagenesis; transition state

The importance of macromolecular recognition in guiding a large number, if not the majority, of cellular metabolic processes such as signal transduction, apoptosis, transcription, cell to cell communication, protein folding, etc., is becoming increasingly appreciated. The understanding of protein recognition is, at present, predominantly qualitative; however, a number of careful investigations on the thermodynamics and kinetics of these reactions have been published (Altschuh et al., 1992; Foote & Winter, 1992; Sancho & Fersht, 1992; Schreiber & Fersht, 1995; England et al., 1997). These interactions require the establishment of contacts typically between 10–20 individual amino acids from each interacting partner (Janin & Chothia, 1990). Site-directed mutagenesis studies have begun to probe their relative contributions (e.g., Wells, 1991; Jin & Wells, 1994; Clackson & Wells, 1995; Schreiber & Fersht, 1995; Dall'Acqua et al., 1996).

The role of protein–protein interactions has been extensively studied with components of the immune system. X-ray structures of the complexes have guided kinetic and site-directed mutagenesis investigations of several protein antigen–antibody complexes, including that of the chicken lysozyme specific monoclonal antibody, D1.3 (England et al., 1997).

The lysozyme (HEWL)·HyHEL-10 Fab (Fab-10) complex was characterized by Padlan et al. (1989), and free energy contributions of the chicken lysozyme epitope residues Asn19, Arg21, Asp101, and Gly102 were evaluated by extensive amino acid replacements (Kam-Morgan et al., 1993). Replacements of several HyHEL-10 Fv paratope residues have also been thermodynamically investigated (Tsumoto et al., 1995, 1996). Methods are presented in the present study that allow determination of the kinetics describing

Reprint requests to: Jack F. Kirsch, Department of Molecular and Cell Biology, University of California, 229 Stanley Hall, Berkeley, California 94720; e-mail: jfkirsch@uclink4.berkeley.edu.

[4]Present address: Dade Behring Incorporated, Research Department, San Jose, California 95135.

Abbreviations: HEWL, hen (chicken) egg-white lysozyme (EC 3.2.1.17); Fab-10, Fab fragment of the HyHEL-10 monoclonal antibody; WT, wild-type lysozyme; K_D, dissociation constant for the lysozyme·antibody complex; ΔG_D, the corresponding free energy of dissociation; k_{on} and k_{off}, association and dissociation rate constants, respectively, for interaction of the lysozyme and antibody; $\Delta G^{\ddagger}_{on}$ and $\Delta G^{\ddagger}_{off}$, the corresponding activation energies of association and dissociation, respectively; subscripts L and H, antibody light and heavy chain, respectively.

the formation and decomposition of mutant HEWL·WT Fab-10 complexes. The association rate constants are monitored by the decrease in activity associated with the formation of the nearly inactive HEWL·WT Fab-10 complex. The ratios of the difference activation energies of formation, $\Delta\Delta G^{\ddagger}_{on}({}^{MUT}\Delta G^{\ddagger}_{on} - {}^{WT}\Delta G^{\ddagger}_{on})$ to the difference free energies of dissociation, $\Delta\Delta G_D({}^{WT}\Delta G_D - {}^{MUT}\Delta G_D)$, are referred to as Φ values, a parameter related to the β values of the Brønsted relationship, and introduced by Fersht and colleagues to evaluate transition state structures in protein folding studies (Sancho et al., 1991; Fersht et al., 1992; Horovitz & Fersht, 1992; Matouschek et al., 1992; Sancho & Fersht, 1992; Serrano et al., 1992a, 1992b, 1992c). The large data set of individual site replacements allows the determination of two sets of Φ values describing the extent of interaction at lysozyme positions 21 and 101 in the transition state of antigen–antibody complex formation.

Results

Wild-type HEWL·Fab-10 complex

The value of K_D for the WT·Fab-10 complex is 75 ± 8 pM (Table 1); therefore, the rates of dissociation of the complexes do not significantly intrude into the kinetics, for all but the weakest complexes, because [Fab-10] was generally $\gg K_D$.

The value of k_{on} for the WT·Fab-10 complex formation is 1.49 ± 0.07 × 10^6 M^{-1} s^{-1}. Dissociation rate constants can be calculated from the independently determined values for K_D and k_{on} as $k_{off} = k_{on}/K_D$, or measured independently as described in Rajpal et al. (1998). Smith-Gill et al. (pers. obs.) measured k_{on} and k_{off} values of 0.23 × 10^6 M^{-1} s^{-1} and 0.52 × 10^{-4} s^{-1}, respectively, for the WT HEWL reaction with HyHEL-10, by surface plasmon resonance analysis at pH 7.4 with 150 mM NaCl added. The calculated K_D is 220 pM.

Aspartate 101 mutants

Asp101 makes a hydrogen bond with $Tyr53_H$ on the Fab-10 heavy chain (Padlan et al., 1989) (Fig. 1c). Equilibrium constants for the substituted Asp101 HEWL·Fab-10 complexes were determined by Kam-Morgan et al. (1993).

The constants describing the equilibria and kinetics of the interactions of Fab-10 with WT and mutant lysozymes are given in Table 1. The WT HEWL + Fab-10 association rate constant is 1.49 ± 0.07 × 10^6 M^{-1} s^{-1}. The mutations at position 101_{HEWL} resulted in 1.5–8.4-fold decreases in the value of this rate constant. There may be a slight inverse correlation of the corresponding $\Delta\Delta G^{\ddagger}_{on}$ values with side-chain volume (Richards, 1974; Creighton, 1993) that becomes more apparent when this quantity is greater than 80 Å^3 (Fig. 2a). The negatively charged D101E mutant associates with the antibody with a rate constant that approaches that observed with WT lysozyme. A plot of the calculated $\Delta\Delta G^{\ddagger}_{off}$ values for position 101_{HEWL} mutant complexes versus side-chain volumes is shown in Figure 2B.

Arginine 21 mutants

Kam-Morgan et al. (1993) found that most Arg21 substitutions, presumably disrupting hydrogen bonds to two antibody tyrosine residues (see Discussion), resulted in a net loss of 2.2 kcal/mol in $\Delta\Delta G_D$ compared to the WT HEWL complex (Fig. 3, dotted line). The R21A·Fab-10 complex, however, is only 0.82 ± 0.08 kcal/mol less stable than that formed from WT HEWL. The R21M·Fab-10 $\Delta\Delta G_D$ of 2.1 kcal/mol fits the earlier correlation (Rajpal et al., 1998).

The rate constants for the association of all Arg21 mutant lysozymes with Fab-10 are about twofold (range: 1.3- to 2.7-fold) less than that exhibited by the WT protein except for R21E (5.2-fold lower) and R21A (nearly identical to that of WT HEWL) (Fig. 4a). A plot of the calculated $\Delta\Delta G^{\ddagger}_{off}$ values for position 21_{HEWL} mutant complexes versus side chain volumes is shown in Figure 4b.

Lysine 97 mutants

The only ion pair in the complex is formed from Lys97 of lysozyme and $Asp32_H$ of Fab-10 (Fig. 1b) (Padlan et al., 1989) (see Discussion). Six substitutions at position 97_{HEWL} were produced to explore the quantitative contribution of this interaction. Replacement with methionine (K97M) resulted in a $\Delta\Delta G_D$ of only 0.80 ± 0.15 kcal/mol (Table 1). The arginine replacement, K97R, forms a substantially weaker complex ($\Delta\Delta G_D$ = 3.05 ± 0.32 kcal/mol).

The values of the $\Delta\Delta G_D$ for the position 97_{HEWL} mutants are dominated by the size of the side chain with a $\Delta\Delta G_D$ of 6.4 kcal/mol between the WT and K97G complexes (Fig. 3). These results contrast sharply with the shallow dependencies observed earlier for substitutions at positions 101_{HEWL} and 21_{HEWL} (Fig. 3, dashed and dotted lines, respectively). The values of k_{on} could only be determined for formation of the K97E, M, and R complexes because the high K_D values for the K97G, A, and D complexes make it difficult to drive the reactions to completion.

Other mutants

Lysine 96 is hydrogen bonded to the side chain carbonyl oxygen of the antibody $Asn31_L$ (Fig. 1b) and to the main chain of His15 in HEWL (Padlan et al., 1989). Lys96 is also within contact distance of $Tyr50_L$. The relatively conservative mutation, K96M, results in a substantial, 6.8 kcal/mol (Table 1), decrease in affinity for the antibody providing clear evidence for the dominance of the ϵ-NH_3^+ interactions at this position.

The unrefined X-ray structure of the HEWL·Fab-10 complex raises the possibility that Tyr20 of lysozyme may form a long hydrogen bond with the main-chain carbonyl oxygen of $Ser91_L$ ($r_{O\text{-}O}$ = 3.4 Å) (Padlan et al., 1989). The resultant Y20F mutant has about the same affinity and indistinguishable kinetics for antibody as WT lysozyme (Table 1); therefore, the postulated hydrogen bond does not contribute significantly to the free energy of association.

The main-chain amide nitrogen of Gly102 forms a hydrogen bond with the side-chain phenolic oxygen of $Tyr58_H$ ($r_{N\text{-}O}$ = 2.6 Å) (Padlan et al., 1989). Replacement of this group with valine, the WT residue in Japanese Quail lysozyme, resulted in small changes in rate constants and equilibria (Table 1), showing that the increased steric hindrance of the larger valine side chain does not significantly effect association.

Discussion

General characteristics of protein–protein interactions

Protein–protein interfaces are characterized by interacting surfaces with combined areas of 1,150–3,300 Å^2 (Janin, 1995, 1997). The

Table 1. *Equilibrium and rate constants describing the interaction of Fab-10 with HEWL variants*[a]

HEWL variant	K_D (nM) ($\Delta\Delta G_D$) (kcal/mol)	k_{on} (10^6 M^{-1} s^{-1}) ($\Delta\Delta G^{\ddagger}_{on}$) (kcal/mol)	k_{off}[b] (10^{-4} s^{-1}) ($\Delta\Delta G^{\ddagger}_{off}$) (kcal/mol)
WT	0.075 ± 0.008[c] (0.00)[d]	1.49 ± 0.07 (0.00)[d]	1.12 ± 0.13 (0.00)[d]
R21G	5.8 ± 2.5[c] (2.57 ± 0.26)	1.00 ± 0.06 (0.24 ± 0.05)	58 ± 25 (0.09 ± 0.02)
R21A	0.30 ± 0.03[e] (0.82 ± 0.08)	1.47 ± 0.04[e] (0.01 ± 0.03)	4.4 ± 0.5 (0.81 ± 0.09)
R21N	5.0 ± 0.8[c] (2.48 ± 0.11)	0.92 ± 0.05 (0.29 ± 0.04)	45 ± 8 (2.19 ± 0.12)
R21E	6.2 ± 1.5[c] (2.61 ± 0.16)	0.29 ± 0.02 (0.98 ± 0.05)	18 ± 4 (1.63 ± 0.16)
R21Q	5.6 ± 1.4[c] (2.55 ± 0.16)	1.02 ± 0.05 (0.22 ± 0.04)	58 ± 15 (2.33 ± 0.17)
R21H	3.8 ± 1.7[c] (2.32 ± 0.26)	1.14 ± 0.12 (0.16 ± 0.07)	44 ± 19 (2.17 ± 0.27)
R21M	2.39 ± 0.13 (2.05 ± 0.07)	0.60 ± 0.01 (0.54 ± 0.03)	14.3 ± 0.8 (1.51 ± 0.07)
R21K	1.9 ± 0.6[c] (1.92 ± 0.20)	0.79 ± 0.07 (0.38 ± 0.06)	15 ± 5 (1.55 ± 0.21)
R21W	3.6 ± 1.3[c] (2.28 ± 0.23)	0.56 ± 0.04 (0.58 ± 0.05)	20 ± 8 (1.70 ± 0.23)
K97G	3,900 ± 500[f] (6.41 ± 0.10)	N.D.[g]	N.D.[g]
K97A	890 ± 150[f] (5.74 ± 0.12)	N.D.[g]	N.D.[g]
K97D	6,900 ± 1,500[f] (6.75 ± 0.14)	N.D.[g]	N.D.[g]
K97E	33 ± 6 (3.59 ± 0.12)	0.45 ± 0.03 (0.71 ± 0.04)	150 ± 30 (2.88 ± 0.13)
K97M	0.29 ± 0.07 (0.80 ± 0.15)	0.57 ± 0.04 (0.56 ± 0.05)	1.7 ± 0.4 (0.24 ± 0.16)
K97R	13 ± 7 (3.05 ± 0.32)	0.62 ± 0.04 (0.52 ± 0.05)	82 ± 43 (2.54 ± 0.32)
D101G	0.18 ± 0.08[c] (0.53 ± 0.27)	0.59 ± 0.02 (0.55 ± 0.03)	1.1 ± 0.5 (−0.02 ± 0.27)
D101A	0.98 ± 0.25[c] (1.52 ± 0.16)	0.63 ± 0.15 (0.51 ± 0.14)	6 ± 2 (1.01 ± 0.21)
D101S	2.3 ± 0.4[c] (2.02 ± 0.12)	0.43 ± 0.02 (0.73 ± 0.04)	10 ± 2 (1.29 ± 0.13)
D101N	1.2 ± 0.4[c] (1.65 ± 0.21)	0.50 ± 0.04 (0.65 ± 0.05)	6.0 ± 2.1 (1.00 ± 0.21)
D101E	3.6 ± 0.8[c] (2.28 ± 0.14)	1.02 ± 0.08 (0.22 ± 0.05)	36 ± 8 (2.06 ± 0.15)
D101Q	3.3 ± 0.8[c] (2.23 ± 0.15)	0.56 ± 0.04 (0.58 ± 0.05)	18 ± 5 (1.65 ± 0.16)
D101K	3.5 ± 0.8[c] (2.27 ± 0.15)	0.32 ± 0.04 (0.91 ± 0.07)	11 ± 3 (1.36 ± 0.16)
D101F	5.0 ± 1.5[c] (2.48 ± 0.19)	0.18 ± 0.02 (1.25 ± 0.06)	9 ± 3 (1.22 ± 0.20)
D101R	4.6 ± 1.7[c] (2.44 ± 0.23)	0.27 ± 0.04 (1.00 ± 0.08)	13 ± 5 (1.44 ± 0.24)
Other mutations			
Y20F	0.032 ± 0.001[e] (−0.51 ± 0.06)	1.92 ± 0.03[e] (−0.15 ± 0.03)	0.61 ± 0.01 (−0.36 ± 0.07)
K96M	7,000 ± 1,200[f] (6.76 ± 0.12)	N.D.[g]	N.D.[g]
G102V	0.19 ± 0.04[c] (0.55 ± 0.14)	0.54 ± 0.02 (0.59 ± 0.03)	1.0 ± 0.2 (−0.05 ± 0.14)

[a]The determination of K_D and k_{on} values is described in Materials and methods. All reactions were performed in 66 mM potassium phosphate buffer, pH 6.24, 25 °C.

[b]Calculated from K_D and k_{on} values.

[c]Some of these values differ slightly from those reported earlier (Kam-Morgan et al., 1993) because of the inclusion of the results from additional measurements.

[d] $^{WT}\Delta G_D = -13.78 \pm 0.06$ kcal/mol; $^{WT}\Delta G^{\ddagger}_{on} = 9.01 \pm 0.03$ kcal/mol; $^{WT}\Delta G^{\ddagger}_{off} = 22.78 \pm 0.07$ kcal/mol.

[e]From Rajpal et al. (1998).

[f]These data were obtained by partial forcing of the fitted curve to the blank rate as the end point. This procedure was adopted for the lowest affinity mutants because of the limited availability of Fab-10.

[g]N.D., not determined.

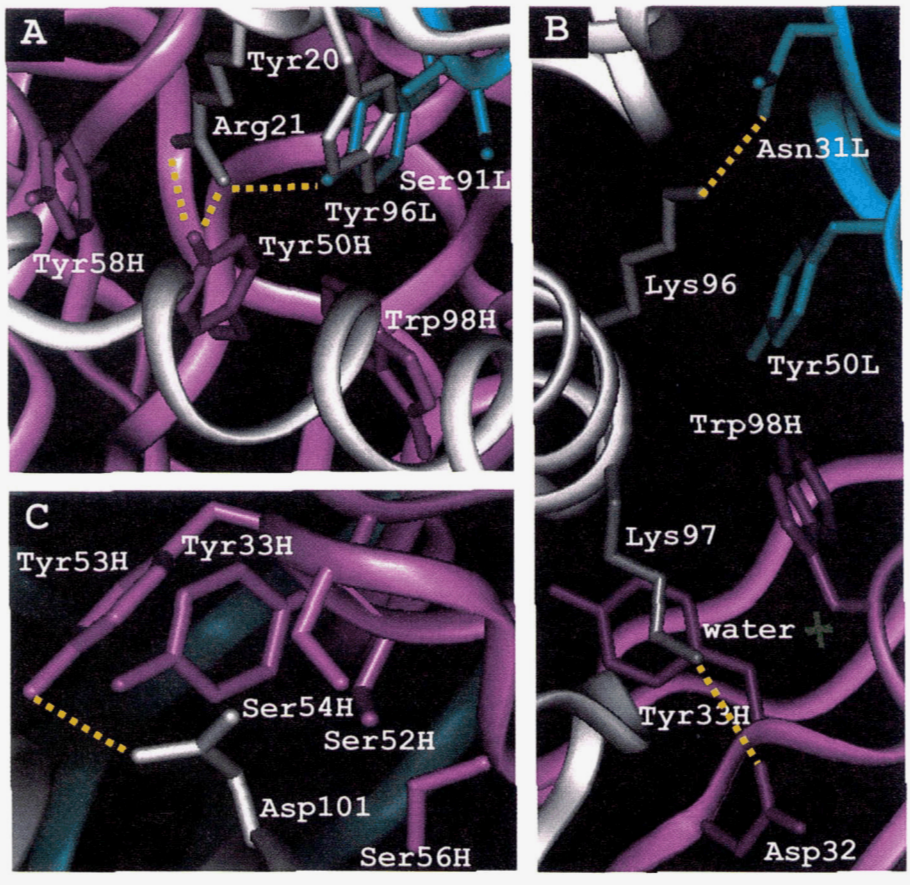

Fig. 1. Schematic view of the interactions of HEWL residues (**A**) Tyr20 and Arg21, (**B**) Lys96 and Lys97, and (**C**) Asp101 with corresponding residues of Fab-10 in the crystallographically determined epitope (PDB code 3HFM; Padlan et al., 1989). Lysozyme residues are shown in silver. Fab-10 heavy and light chain residues are shown in magenta and light blue, respectively. The only crystallographically observable water in **B** is shown in green.

free energies of association, ΔG_D, for these protein complexes cover a wide range: (−4.8 to −19.4 kcal/mol; reviewed by Horton & Lewis, 1992; see also Braun et al., 1988). Antibody–protein antigen complexes typically involve buried surface areas of 1,250–1,950 Å^2 (Janin, 1995).

Intermolecular contacts in protein–protein interfaces include hydrogen bonds, electrostatic, and van der Waals interactions. Bound solvent molecules are released (Bhat et al., 1994), and decreases in the conformational entropies of interacting side chains ensue upon association. The relative contributions of each of these factors is likely to be system dependent.

Association rate constants, k_{on}, are 10^5–10^9 M^{-1} s^{-1} (reviewed by Janin & Chothia, 1990; see also Schreiber & Fersht, 1995; Janin, 1997), but the range is smaller for monoclonal antibody–protein antigen complexes: 10^5–10^6 M^{-1} s^{-1} (Friguet et al., 1989; Janin & Chothia, 1990; Foote & Winter, 1992; Raman et al., 1992; Janin, 1995; Glaser & Hausdorf, 1996; England et al., 1997). The variation within the K_D values is thus primarily due to the large range in the corresponding dissociation rate constants (1–10^{-7} s^{-1}) (Janin & Chothia, 1990). As a result, mutations that perturb the various residue–residue contacts predominantly effect k_{off}, with considerably less effect on k_{on}, although a contrary example has recently been observed (Smith-Gill et al., pers. obs.).

Methodology

The determination of the K_D values for the complexes of Fab-10 with WT and mutant HEWLs in *homogeneous* solution was enabled by the fact that this antibody occludes the active site of the enzyme, so that the extent of complex formation parallels the decrease in activity (Kam-Morgan et al., 1993). The fully associated complex does exhibit about 5% of WT activity in the *Micrococcus luteus* cell wall assay (Shugar, 1952). This residual activity was usually ignored in the analysis, but inclusion sometimes improved the fit of the data to the calculated curves generated by the models (Equation 2 of Rajpal et al., 1998).

Similarly, advantage was taken of the decrease in activity associated with complex formation to determine the value of the association rate constant. The rate law is given in Equation 1 in Materials and methods, and the derivation is in the Appendix.

Surface plasmon resonance is a generally applied method for measuring the rate constants for protein–protein interactions, because of its wide applicability and ease of use. This method requires that one of the two components of the reaction mixture be immobilized while the second flows over that surface. Thus, this is a heterogeneous, as opposed to a homogeneous, system with associated limitations. Schuck and Minton (1996) discussed exam-

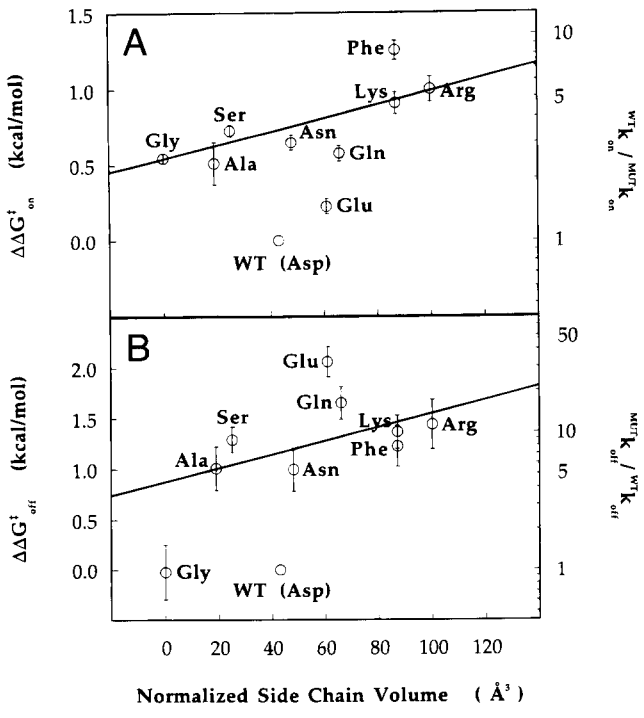

Fig. 2. The kinetics of the HEWL·Fab-10 reactions as influenced by amino acid replacements at position 101_{HEWL}. **A:** Relative association rate constants, k_{on} (right ordinate), and derived difference free energies, $\Delta\Delta G^{\ddagger}_{on}$ (left ordinate) ($\Delta\Delta G^{\ddagger}_{on} = {}^{MUT}\Delta G^{\ddagger}_{on} - {}^{WT}\Delta G^{\ddagger}_{on}$). **B:** Relative dissociation rate constants, k_{off} (right ordinate), and derived difference free energies, $\Delta\Delta G^{\ddagger}_{off}$ (left ordinate) ($\Delta\Delta G^{\ddagger}_{off} = {}^{WT}\Delta G^{\ddagger}_{off} - {}^{MUT}\Delta G^{\ddagger}_{off}$).

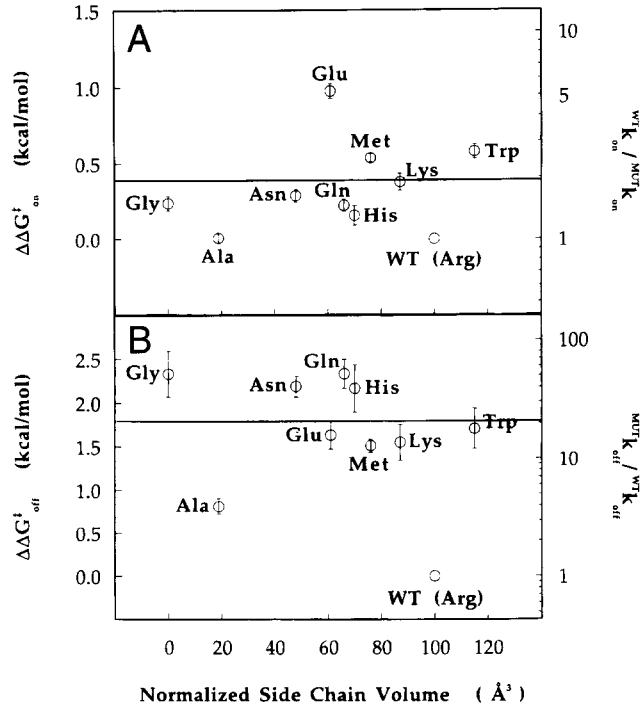

Fig. 4. The kinetics of the HEWL·Fab-10 association reaction as influenced by side-chain volume of the amino acid replacements at position 21_{HEWL} (for key, see legend for Fig. 2).

ples where the independently determined values of K_D significantly differ from the ratios of dissociation and association rate constants determined by biosensor methods. Multivalency, nonspecific binding, antigen (or antibody) rebinding, poor mass transport due to insufficient reagent flow rates, and steric hindrance within immobilized protein surfaces can result in apparent affinity and kinetic constants that have no direct relationship to those determined in homogeneous solution (Nieba et al., 1996; Sadana & Chen, 1996; England et al., 1997).

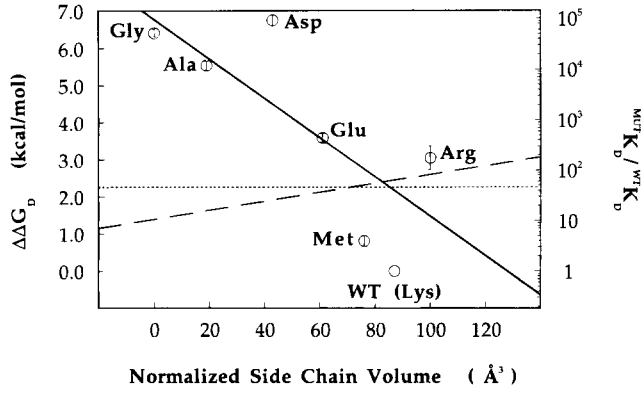

Fig. 3. Effect of side-chain volume of the amino acid replacement on the difference free energies of dissociation ($\Delta\Delta G_D = {}^{WT}\Delta G_D - {}^{MUT}\Delta G_D$) of Fab-10 with HEWL. The data points (open circle) with error bars are for replacements at position 97_{HEWL} (WT = Lys). The trend line (—) for mutations at position 97_{HEWL} is shown (no theoretical significance). The trend lines representing mutations at positions 21_{HEWL} (WT = Arg) and 101_{HEWL} (WT = Asp) (··· and – –, respectively) of HEWL are from Kam-Morgan et al. (1993), and the data are shown in that paper. All data were collected at pH 6.24, in 66 mM potassium phosphate buffer, 25 °C.

Aspartate 101

Crystallographic studies suggest that Asp101 is hydrogen bonded to the antibody residue, $Tyr53_H$, as well as being within contact distance of $Tyr33_H$, $Ser52_H$, $Ser54_H$, and $Ser56_H$ (Padlan et al., 1989) (Fig. 1c). In addition, the main-chain carbonyl oxygen of $Tyr53_H$ is within 2.3 Å of a carboxylate oxygen atom of Asp101; a presumably unfavorable contact. Comparison of the structures of free and complexed lysozyme established that Asp101 undergoes significant rearrangement upon binding to Fab-10.

Substitution of Asp101 with other amino acids leads to decreases in the stabilities in the corresponding HEWL·Fab-10 complexes that are well correlated with increasing side-chain volume. The slope = 0.012 ± 0.002 kcal/mol/Å^3, for example, the $\Delta\Delta G_D$'s of the D101A and D101F complexes from that of WT are 1.5 and 2.5 kcal/mol, respectively (Kam-Morgan et al., 1993) (Fig. 3). The WT·Fab-10 complex is 1.6 kcal/mol more stable than predicted from the regression line in Figure 1 of Kam-Morgan et al. (1993), showing the importance of additional factors, such as optimal electrostatic and nonpolar interactions.

The dependence of the values of k_{on} upon side-chain volume in the 101 series is very slight (Table 1; Fig. 2A). Most mutations elicit only an approximately threefold drop in this rate constant, while slightly larger decreases were observed with those mutations

that substitute larger side chains (i.e., D101K, D101F, or D101R). The k_{on} value for formation of the D101E complex is only decreased by one-third compared to WT. This might have been expected from the retention of the anion in the side chain; however, k_{off} for the D101E complex is anomalously large (see below).

The slope of 0.0045 ± 0.0005 kcal/mol/Å^3, correlating the values of $\Delta\Delta G^{\ddagger}_{on}$, is a little smaller than that of 0.0067 ± 0.0021 kcal/mol/Å^3 for $\Delta\Delta G^{\ddagger}_{off}$. Thus, more of the mutational induced change in $\Delta\Delta G_D$ in this series is reflected in the dissociation rate constants. This appears to be the more common observation in mutational analyses of protein/protein interactions (e.g., Friguet et al., 1989; Foote & Winter, 1992; Schreiber & Fersht, 1995; England et al., 1997).

The value of k_{off} for the D101E complex is significantly larger than that predicted from the correlation line of Figure 2B. This is unexpected, given the retention of the negative charge. The value of K_D for the D101G complex is nearly indistinguishable from that of WT (Kam-Morgan et al., 1993), as is the corresponding value of k_{off} (Table 1).

Arginine 21

The quanidinium side chain of Arg21 forms hydrogen bonds with the antibody residues, Tyr96$_L$ and Tyr50$_H$ (Padlan et al., 1989) (Fig. 1A). The main-chain amide moiety of Arg21 also hydrogen bonds to the main-chain carbonyl oxygen of Asn92$_H$. Arg21 is also within contact distance of residues Tyr58$_H$ and Trp98$_H$.

Most substitutions at position 21$_{HEWL}$ studied by Kam-Morgan et al. (1993) (R21G, N, E, Q, and W) destabilize the resultant complexes by about 2.2 kcal/mol relative to the WT complex; a pattern very different from that observed at position 101$_{HEWL}$ (Fig. 3). Only the cationic amino acid substitutions, R21K and R21H, exhibited any deviation from this pattern, consistent with a small partial restoration of the overall binding energy (Kam-Morgan et al., 1993). A current analysis of the stabilities of the R21A, M, and V complexes found additionally that the stability of the complex is inversely proportional to the size of the aliphatic side chain (Rajpal et al., 1998).

Most mutations at position 21$_{HEWL}$ result in 30–60% reductions in the value of k_{on} for complex formation. These observations contrast with those recorded for mutations in the F_v for the WT HEWL·D1.3 complex where unchanged values or small increases in k_{on} were mostly observed (Ito et al., 1995; England et al., 1997). The value of k_{on} for formation of the R21A complex is identical to that of WT, an observation that by itself might be interpreted as countering the view that long-range electrostatic forces are important in determining the values of k_{on} (Kozack & Subramanian, 1993; Van Oss, 1995). Charge reversal at this position (R21E), however, introduces the largest decrease of k_{on} introduced in this series (80%). There are insufficient data in the literature to generalize on this point.

The general rule that the effects of mutations are most pronounced in the rate constants for the dissociation of protein–protein complexes is obeyed in the Arg21 series. The increases in k_{off} range from threefold for the R21A complex to above 50-fold in the R21Q complex. There is no correlation with charge type as the R21K, M, and E complexes dissociate with nearly the same rate constants.

Lysine 97

Only one intermolecular salt bridge is observed in the X-ray structure of the HEWL·Fab-10 complex (Padlan et al., 1989). It is between Lys97 and Asp32$_H$ (Fig. 1B). Lys97 is also in van der Waals contact with Tyr33$_H$ and Trp98$_H$. These authors suggested that the large distance between the charged atoms (3.6 Å) and the presence of a single water molecule in van der Waals contact with the ϵ-amino group of Lys97 would tend to reduce the contribution of this charge–charge interaction to the overall binding energy.

Substitutions at position 97$_{HEWL}$ result in as much as five orders of magnitude decrease in antibody affinity relative to WT HEWL contrasting with the position 101$_{HEWL}$ and 21$_{HEWL}$ results (Fig. 3). In general, the $\Delta\Delta G_D$ values increase as the side-chain volume of the substituted residue deviates from that of the original lysine. That is, the smallest residue replacements (K97G, K97A, and K97D) yield the largest losses in free energy of association (6.41 ± 0.10, 5.54 ± 0.12, and 6.75 ± 0.14 kcal/mol, respectively). The K97M mutant, which was generated to remove the positive charge with minimum effect on the rest of the side chain, produced only a minor destabilization in the free energy of complex formation ($\Delta\Delta G_D$ = 0.80 ± 0.15 kcal/mol). This small value is not unexpected in light of a recent study in which Asp32$_H$ was mutated to an asparagine, resulting in the loss of the same ion pair, with little effect on affinity ($\Delta\Delta G_D$ = 0.40 ± 0.25 kcal/mol) (Tsumoto et al., 1996). The K97R mutation, which preserves the positive charge at this position, results in a moderate destabilization relative to the WT complex, further illustrating the minimal contribution of the cation in this charge–charge interaction.

A computational analysis of a variety of salt bridges demonstrated that molecular modeling replacement of charged residues with hydrophobic isosteres often results in more favorable free energy of association (Hendsch & Tidor, 1994). They suggested further that the role of salt bridges may be to increase specificity at the expense of excess free energy of association.

The changes in the rate constants associated with the K97M complex are an interesting exception to the general tendency of free energy changes to be reflected predominantly in k_{off}. The value of k_{off} in this case is, within error, not much changed from that of the WT complex, while that for k_{on} is decreased nearly threefold (Table 1).

Transition state structures for protein docking

The elegant, modified Brønsted, protein engineering approach to the experimental determination of transition state structures in protein folding reactions, developed by Fersht and his associates, can be extended to protein–protein interactions. The analysis measures the effect of a series of mutations at a given position on the ratio:

$$\Phi_{unf} = \frac{\Delta\Delta G^{\ddagger}_{unf}}{\Delta\Delta G^{unf}_{eq}}$$

where $\Delta\Delta G^{\ddagger}_{unf}$ is the difference in free energy of activation for the unfolding rate constant of the mutant versus the wild-type protein, and $\Delta\Delta G^{unf}_{eq}$ is the corresponding difference in the total free energy of unfolding. A value of Φ_{unf} = 0 indicates that the residue in question lies in an environment in the transition state that closely resembles that of the folded state, while a value of Φ_{unf} = 1 implies the converse (Sancho et al., 1991; Fersht et al., 1992; Horovitz & Fersht, 1992; Matouschek et al., 1992; Sancho & Fersht, 1992; Serrano et al., 1992a, 1992b, 1992c).

We can describe two general models for protein association. In the first, the process is resolved notionally into the two steps

shown in Figure 5. The first is the formation of an encounter complex that is relatively unpopulated compared to the reactant and transition states. This species is characterized by the loss of three degrees each of translational and rotational entropy accompanying "2 → 1" association reactions. These entropy losses are in part offset by introduced vibrations specific to the complex (Jencks, 1981). The components of such a complex as envisioned would largely retain the solvation shells of the individual proteins, and few of the short-range interactions of the docked complex would be established (Van Oss, 1995). The second step is the annealing process, in which the solvent structure of the interface is formed, short-range hydrophobic, hydrogen bond, and electrostatic interactions are made, and conformational changes achieved both at the epitope–paratope interface as well as at remote sites (Williams et al., 1996).

We extend the Φ value concept to protein–protein interactions by the formula:

$$\Phi = \frac{\Delta\Delta G^{\ddagger}_{on}}{\Delta\Delta G_D}.$$

According to this model, a Φ value near zero, i.e., where the effect of a series of mutations at a single site on the association rate constants is very small compared to those on the overall equilibrium constant, is characteristic of a docking transition state where the first step, i.e., formation of the encounter complex at this site, is rate determining, and annealing steps are rapid compared to complex dissociation. This is so, because single site mutations would be expected to have negligible effects on the physics of diffusion. Larger values of Φ signal increasing contributions from the annealing process. Different Φ values can be associated with each site on the protein, and can be used to provide information about the docking trajectory.

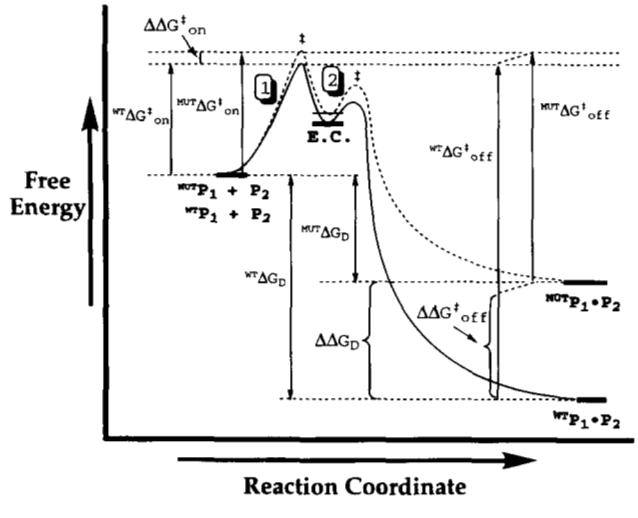

Fig. 5. Reaction coordinate diagram describing a protein–protein interaction ($P_1 + P_2 \rightarrow P_1 \cdot P_2$). Most mutations have little effect on the association rate constant, while the majority of the effect in $\Delta\Delta G_D$ is reflected in $\Delta\Delta G^{\ddagger}_{off}$. The dip in the profile represents the encounter complex (E.C.) (see Janin, 1997). Step 1, encounter complex formation is the highest barrier at those epitope sites with low Φ values, while step 2, annealing of the encounter complex, is a significant kinetic barrier at those positions with larger Φ values (see Discussion).

A simpler, but physically unlikely, model involves a single transition state, where all interactions reach their greatest free energy barrier height at the same fractional extent of the reaction. This model, which allows no metastable intermediates, is extremely improbable for such a complicated process involving the establishment of numerous intermolecular contacts and solvation changes. The Φ values in this second model provide a measure of the extent of bond making at each site in the transition state.

The preponderance of the experimental data presented here and in the cited references shows that the effects of mutation are largely realized in the values of k_{off}; therefore, the transition state for docking in most cases, is early (step 1 of Fig. 5). Implementation of the Brønsted analysis requires that a statistically large number of substituents be introduced at each probed position, and that the majority of these *at this site* generate similar Φ values. Outliers in a series will be found occasionally; i.e., the Φ value for a given substitution at a particular site is significantly different from the average Φ value for the others at this site. This can occur as a result of division of small $\Delta\Delta G^{\ddagger}_{on}$ by a small $\Delta\Delta G_D$, leading to a large apparent error, and an artifactual deviation. Alternatively, a given mutation can effect the energetics at remote sites. This outcome may sometimes be distinguished by double mutant cycle analysis (Carter et al., 1984; Goldman et al., 1997). The present work, to the best of our knowledge, is the first to present sufficient accumulated experimental data to permit a Brønsted analysis of protein–protein interactions.

Φ *Values at specific sites*

Replacement of Arg21 with glycine, asparagine, glutamine, or histidine gave Φ values ranging from 0.01–0.12, while the larger lysine, methionine, and tryptophan resulted in slightly higher Φ values of 0.20–0.26 (Table 2; Fig. 6A). The weighted average for these seven replacements is 0.14 ± 0.03. These combined data argue that the environment of Arg21 in the docking transition state is very close to what it is in free lysozyme and that specific interactions made with, for example, $Tyr96_L$ and $Tyr50_H$ follow in post rate-determining steps. That is, the rate-determining step is the formation of the encounter complex as experienced by this site. The R21E mutation results in a higher Φ value of 0.37 consistent with a substantial kinetic barrier contribution from the annealing step for this charge reversal mutation.

Accurate Φ values could be determined only for the K97E and K97R mutations at this position (Table 2). Both of these values are about 0.2, despite the opposite charges. The transition state is early in this, as in the position 21_{HEWL} series. The apparent Φ value for the K97M mutation of 0.7 may be unreliable, due to the large associated error.

The largest number, nine, of Φ values were determined at position 101_{HEWL} (Table 2; Fig. 6B). That for D101G is unreliable because of the small perturbation in $\Delta\Delta G$ values. The weighted average of the other seven Φ values, D101E excluded, is a very well defined 0.36 ± 0.03. These results could argue that the transition state experienced at position 101_{HEWL} occurs later on the reaction coordinate than it does for residues at position 21_{HEWL}. The one mutation, however, that conserves the charge, D101E, generates a small Φ value of 0.10 ± 0.02. This figure argues for an early transition state at position 101_{HEWL}. The difference could be a simple manifestation of favorable electrostatic steering that increases the proportion of productive collisions.

Table 2. *Φ values for complexation of Fab-10 with HEWL variants*

HEWL variant	Φ value[a]
WT	N.A.[b]
R21G	0.09 ± 0.02
R21A	0.01 ± 0.04
R21N	0.12 ± 0.02
R21V	N.C.[c]
R21E	0.37 ± 0.03
R21Q	0.08 ± 0.02
R21H	0.07 ± 0.03
R21M	0.26 ± 0.02
R21K	0.20 ± 0.04
R21W	0.25 ± 0.03
Position 21_{HEWL} average[d]	0.14 ± 0.03
K97E	0.20 ± 0.01
K97M	0.70 ± 0.15
K97R	0.17 ± 0.02
Position 97_{HEWL} average[e]	—
D101G	1.04 ± 0.54
D101A	0.34 ± 0.06
D101S	0.36 ± 0.03
D101N	0.39 ± 0.06
D101E	0.10 ± 0.02
D101Q	0.26 ± 0.03
D101K	0.40 ± 0.04
D101F	0.51 ± 0.05
D101R	0.41 ± 0.05
Position 101_{HEWL} average[f]	0.36 ± 0.03

[a]Calculated, as follows: $\Phi = \Delta\Delta G^{\ddagger}_{on}/\Delta\Delta G_D$.
[b]N.A., not applicable.
[c]N.C., not calculable (due to insufficient data).
[d]Weighted average of all position 21_{HEWL} Φ values except R21A, R21E, and R21V (see Discussion for explanation).
[e]This is not a reliable value because of too little data.
[f]Weighted average of all position 101_{HEWL} Φ values except D101G and D101E (see Discussion for explanation).

A few mutations were made at positions 20_{HEWL}, 96_{HEWL}, and 102_{HEWL} (Table 1), but accurate Φ values could not be determined for experimental reasons.

Why are Φ values so small in protein–protein interactions?

The rates of formation of protein–small molecule complexes are generally fast, and often approach diffusion controlled limits (Brouwer & Kirsch, 1982). Specific association rate constants at defined sites can be reduced significantly from the 10^8–10^9 M^{-1} s^{-1} expected for diffusion-controlled reactions by a variety of factors including restricted solid angle geometry (Solc & Stockmayer, 1973), conformational changes in which the substrate reacts with a minor conformer, association coupled with pre-organization or desolvation of the binding site (Julin & Kirsch, 1989; Cannon et al., 1996), or association with a minor prototropic form of the enzyme or ligand.

The above considerations do not generally apply to protein–protein interactions. That is, the solid angles of interaction are relatively large and are confined to the surface, and significant conformational changes on association are rare. The fact that the association rate constants are mostly in the 10^5–10^7 M^{-1} s^{-1} range (Janin & Chothia, 1990) suggests that association with a minor prototropic form of one of the protein partners is uncommon. These factors taken together account for the early transition states noted for most protein–protein association reactions. On the other hand, later transition states would be expected for protein association reactions where the chains fold cooperatively (Tsai et al., 1997).

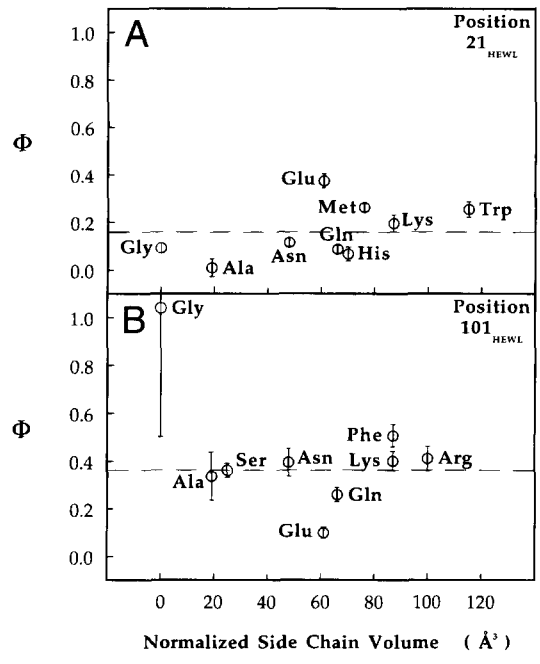

Fig. 6. The effects of side-chain volume of the amino acid replacements at positions (**A**) 21_{HEWL} and (**B**) 101_{HEWL} on Φ values ($\Delta\Delta G^{\ddagger}_{on}/\Delta\Delta G_D$).

Material and methods

Materials

Wild-type HEWL, *M. luteus* (*Micrococcus lysodeikticus*), and corn steep liquor were purchased from Sigma Chemical Company (St. Louis, Missouri). The inactive lysozyme mutant, E35Q, was a gift from Dr. Ichiro Matsumura. Mutants of lysozyme at positions 21_{HEWL}, 101_{HEWL}, and 102_{HEWL} were prepared by Drs. Lei Zhang and Lauren Kam-Morgan. The Fab fragment of HyHEL-10 was prepared by use of the ImmunoPure Fab Kit (Pierce Chemical Company, Rockford, Illinois).

Expression of mutant lysozymes

Site-directed mutagenesis of the hen egg-white lysozyme gene was performed according to Malcolm et al. (1989) with modifications described by Shih et al. (1993) and Matsumura and Kirsch (1996). Expression and purification were carried out according to Kam-Morgan et al. (1993) and Matsumura and Kirsch (1996).

Purification of mutant lysozymes

Cultures were centrifuged at 4,500 × *g* at 4 °C for 10 min to remove cells (lysozyme is excreted into the media). The pH of the

remaining media was raised to 10.7 with concentrated NaOH, followed by centrifugation at 12,000 × *g* at 4 °C for 10 min. The pellet was discarded, and the supernatant was quickly brought to pH 4.7 with concentrated HCl. The crude fraction was diluted 1:1 with distilled de-ionized water and loaded onto an SP-Sepharose column (2.5 × 12 cm) pre-equilibrated with 10 mM KH_2PO_4 (pH 4.7) (Buffer A). The column was washed with 200–300 mL Buffer A and eluted with a gradient from 0–1.5 M NaCl in Buffer A. Active fractions were pooled, concentrated by ultrafiltration using an Amicon YM-10 membrane, and loaded onto a CM-Sepharose column (2.5 × 10 cm) pre-equilibrated with 66 mM potassium phosphate buffer, pH 6.24 (Buffer B). The column was washed with 200–300 mL Buffer B and eluted with 0.5 M NaCl in Buffer B. Active fractions were pooled, and concentrated and desalted using the Centricon-10 microconcentrator. Protein concentrations were determined from $\epsilon_{280} = 38{,}500\ M^{-1}\ cm^{-1}$ (Sophianopoulos et al., 1962).

Determination of antibody concentration

Antibody (or Fab fragment) concentration was determined by titration with WT lysozyme. Aliquots of lysozyme (10 nM = 100 × K_D) were pre-incubated at 25 °C for 1 h with various volumes of added antibody stock solution, and the residual activity monitored by the *M. luteus* assay (Shugar, 1952). The concentration of antibody was determined by extrapolating the volume of added antibody stock solution necessary to effect maximal inhibition of lysozyme activity.

Determination of affinity constants for lysozyme–antibody complexes

Equilibrium constants for the complexes of the active lysozyme forms with either whole HyHEL-10 antibody or the Fab fragment (Fab-10) were determined by the previously described competitive inhibition assay (Kam-Morgan et al., 1993). Fully complexed lysozyme retains approximately 5% of the original enzyme activity. As a result, the equation used by Kam-Morgan et al. (1993) to calculate equilibrium constants has been modified slightly to account for this residual activity (Rajpal et al., 1998).

Determination of the rate constants for the association of lysozyme with antibody

Lysozyme variants (1–4 nM) were mixed with a 5–40 fold molar excess of Fab-10 in the presence of 10–200 μg/mL *M. luteus* cells in Buffer B at 25 °C. Activity was monitored starting 15 s after mixing by the decrease in light scattering at 450 nm. The association rate constant, k_{on}, was calculated by nonlinear regression fit (using either the SAS statistical analysis program; Ray, 1982; or Kaleidagraph™ 3.0) of either the enzyme velocity, v_{obs} (determined at several windows of time) using Equation 1 (see Appendix for derivation):

$$v_{obs} = v_{bl} + \left[\frac{k_{cat}[E_T][S]}{K_m + [S]} \cdot e^{-\left(\frac{k_{on}[Ab_T]K_m t}{K_m + [S]}\right)}\right] \quad (1)$$

or the raw absorbance data, Abs_{obs}, using Equation 2. The latter is the integrated form of Equation 1:

$$Abs_{obs} = Abs_{init} + v_{bl} \cdot t - \left[\frac{k_{cat}[E_T][S]}{k_{on} K_m [Ab_T]} \cdot e^{-\left(\frac{k_{on}[Ab_T]K_m t}{K_m + [S]}\right)}\right] \quad (2)$$

where $[S]$ = initial cell wall substrate concentration, E_T = total lysozyme concentration, Ab_T = total Fab concentration, Abs_{init} = initial absorbance, and v_{bl} = blank velocity (i.e., the nonenzymatic decrease in light scattering with slow time-dependent settling of cell wall particles). The K_m and k_{cat} values used in this analysis were determined independently by nonlinear regression of enzyme activities (in the absence of antibody) from the Michaelis–Menten rate equation. Typically, the k_{on} values were determined from the compiled data for 24 individual reactions.

Propagation of standard error

Propagated standard errors, SEs, are calculated from individual standard errors, as follows:

$$SE_{\Delta G} = RT \cdot \frac{K}{SE_K} \quad (3)$$

$$SE_{\Delta\Delta G} = \sqrt{({}^{WT}SE_{\Delta G})^2 + ({}^{MUT}SE_{\Delta G})^2} \quad (4)$$

where K represents an affinity or rate constant, SE_K refers to the standard error in that constant, ΔG represents the corresponding free-energy term, and $SE_{\Delta G}$ and $SE_{\Delta\Delta G}$ correspond to the propagated standard errors in ΔG and $\Delta\Delta G$, respectively.

The propagated standard error in Φ, SE_Φ, is calculated, as follows:

$$SE_\Phi = \frac{\sqrt{(\Delta\Delta G_D \cdot SE_{\Delta\Delta G^\ddagger_{on}})^2 + (\Delta\Delta G^\ddagger_{on} \cdot SE_{\Delta\Delta G_D})^2}}{(\Delta\Delta G_D)^2}. \quad (5)$$

Appendix

A simplified kinetic scheme for the competition of antibody, Ab, with substrate, S, for the active site of lysozyme, E, is shown below:

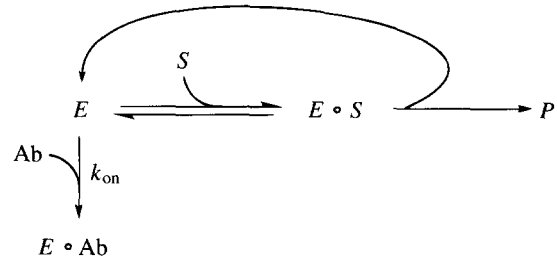

where P and Ab represent the degraded cell wall product and the antibody concentration, respectively. Rates for the enzyme-catalyzed reaction are fast relative to that for antibody association under these conditions (data not shown). The observed decrease in light scattering, v_{obs}, is equal to the rate of product formation plus the rate of nonenzymatic settling of substrate with time, v_{bl}:

$$v_{obs} = v_{bl} + \frac{d[P]}{dt}. \quad (6)$$

The rate of product formation equals the product of the maximum velocity of lysozyme, V_{max}, and the fraction of enzyme that is complexed to substrate:

$$\frac{d[P]}{dt} = V_{\max} \cdot \frac{[ES]}{[E_T]} = k_{\text{cat}}[E_T] \cdot \frac{[ES]}{[E_T]} \tag{7}$$

where E_T equals the total lysozyme concentration (i.e., $E_T = [E] + [ES] + [E\text{Ab}]$). Substituting ($k_{\text{cat}}[E_T]$) for $V_{\max}$ and expanding the fraction of enzyme in the *ES* form gives:

$$\frac{d[P]}{dt} = k_{\text{cat}}[E_T] \cdot \frac{[ES]}{[E] + [ES]} \cdot \frac{[E] + [ES]}{[E_T]}. \tag{8}$$

Note the following:

$$\frac{[ES]}{[E] + [ES]} = \frac{[S]}{K_m + [S]}. \tag{9}$$

Substituting Equation 9 into Equation 8, one gets the following:

$$\frac{d[P]}{dt} = \frac{k_{\text{cat}}[E_T][S]}{K_m + [S]} \cdot \frac{[E] + [ES]}{[E_T]}. \tag{10}$$

Assuming that $k_{\text{off}} \ll k_{\text{on}}[\text{Ab}]$, the time-dependent loss of enzyme that has not complexed with antibody (i.e., $[E] + [ES]$) can be described, as follows:

$$\frac{d([E] + [ES])}{dt} = -k_{\text{on}}[\text{Ab}][E] \tag{11}$$

because only the uncomplexed form of lysozyme, *E*, can associate with antibody. Expanding the $[E]$ term, the following equation can be written:

$$\frac{d([E] + [ES])}{dt} = -k_{\text{on}}[\text{Ab}] \frac{[E]}{[E] + [ES]} ([E] + [ES]). \tag{12}$$

Rearranging Equation 9, one gets the following:

$$\frac{[E]}{[E] + [ES]} = \frac{K_m}{K_m + [S]}. \tag{13}$$

Given experimental conditions in which $[\text{Ab}_T] \gg [E_T]$ (i.e., $[\text{Ab}] \sim [\text{Ab}_T]$, the total antibody concentration), and substituting Equation 13 into Equation 12, the following equation is derived:

$$\frac{d([E] + [ES])}{dt} = -\frac{k_{\text{on}}[\text{Ab}_T]K_m}{K_m + [S]} ([E] + [ES]). \tag{14}$$

Rearranging Equation 14 and integrating results in the following expression:

$$[E] + [ES] = [E_T] \cdot e^{-\left(\frac{k_{\text{on}}[\text{Ab}_T]K_m t}{K_m + [S]}\right)}. \tag{15}$$

Substituting Equation 15 into Equation 10, the following equation is produced:

$$\frac{d[P]}{dt} = \frac{k_{\text{cat}}[E_T[S]}{K_m + [S]} \cdot e^{-\left(\frac{k_{\text{on}}[\text{Ab}_T]K_m t}{K_m + [S]}\right)}. \tag{16}$$

Finally, substituting Equation 16 into Equation 6, one arrives at Equation 1:

$$v_{\text{obs}} = v_{bl} + \left[\frac{k_{\text{cat}}[E_T][S]}{K_m + [S]} \cdot e^{-\left(\frac{k_{\text{on}}[\text{Ab}_T]K_m t}{K_m + [S]}\right)}\right].$$

Acknowledgments

This work was supported by National Institute of General Medical Sciences Postdoctoral Fellowship Award GM14514-01 (M.G.T.) and by the Director, Office of Energy Research, Office of Basic Energy Sciences, Divisions of Materials Sciences and of Energy Biosciences of the United States Department of Energy under Contract No. DE-AC03-76SF00098 to Lawrence Berkeley National Laboratory. We wish to thank Dr. Sandra Smith-Gill for the generous gift of HyHEL-10 IgG and for communication of unpublished results. We appreciate her valuable criticism of the manuscript, as well as that of Dr. Jaume Pons. We are also grateful to Dr. Stephen Holbrook for his assistance with the Insight Program and Silicon Graphics System and to Dr. Jiri Novotny for early access to an unpublished manuscript.

References

Altschuh D, Dubs M-C, Weiss E, Zeder-Lutz G, Van Regenmortel MHV. 1992. Determination of kinetic constants for the interaction between a monoclonal antibody and peptides using surface plasmon resonance. *Biochemistry 31*:6298–6304.

Bhat TN, Bentley GA, Boulot G, Greene MI, Tello D, Dall'Aqua W, Souchon H, Schwarz FP, Mariuzza RA, Poljak RJ. 1994. Bound water molecules and conformational stabilization help mediate an antigen-antibody association. *Proc Natl Acad Sci USA 91*:1089–1093.

Braun PJ, Dennis S, Hofsteenge J, Stone SR. 1988. Use of site-directed mutagenesis to investigate the basis for the specificity of hirudin. *Biochemistry 27*:6517–6522.

Brouwer AC, Kirsch JF. 1982. Investigation of diffusion-limited rates of chymotrypsin reactions by viscosity variation. *Biochemistry 21*:1302–1307.

Cannon WR, Singleton SF, Benkovic SJ. 1996. A perspective on biological catalysis. *Nat Struct Biol 3*:821–833.

Carter PJ, Winter G, Wilkinson AJ, Fersht AR. 1984. The use of double mutants to detect structural changes in the active site of the tyrosyl-tRNA synthetase (*Bacillus stearothermophilus*). *Cell 38*:835–840.

Clackson T, Wells JA. 1995. A hot spot of binding energy in a hormone–receptor interface. *Science 267*:383–386.

Creighton TE. 1993. *Proteins: Structures and molecular properties*, 2nd ed. New York: W.H. Freeman & Company. p 4.

Dall'Acqua W, Goldman ER, Eisenstein E, Mariuzza RA. 1996. A mutational analysis of the binding of two different proteins to the same antibody. *Biochemistry 35*:9667–9676.

England P, Brégégère F, Bedouelle H. 1997. Energetic and kinetic contributions of contact residues of antibody D1.3 in the interaction with lysozyme. *Biochemistry 36*:164–172.

Fersht AR, Matouschek A, Serrano L. 1992. The folding of an enzyme. I. Theory of protein engineering analysis of stability and pathway of protein folding. *J Mol Biol 224*:771–782.

Foote J, Winter G. 1992. Antibody framework residues affecting the conformation of the hypervariable loops. *J Mol Biol 224*:487–499.

Friguet B, Djavadi-Ohaniance L, Goldberg ME. 1989. Polypeptide-antibody binding mechanism: Conformational adaptation investigated by equilibrium and kinetic analysis. *Res Immunol 140*:355–376.

Glaser RW, Hausdorf G. 1996. Binding kinetics of an antibody against HIV p24 core protein measured with real-time biomolecular interaction analysis suggest a slow conformational change in antigen p24. *J Immunol Methods 189*:1–14.

Goldman ER, Dall'Acqua W, Braden BC, Mariuzza RA. 1997. Analysis of binding interactions in an idiotope–antiidiotope protein–protein complex by double mutant cycles. *Biochemistry 36*:49–56.

Hendsch ZS, Tidor B. 1994. Do salt bridges stabilize proteins? A continuum electrostatic analysis. *Protein Sci 3*:211–226.

Horovitz A, Fersht AR. 1992. Co-operative interactions during protein folding. *J Mol Biol 224*:733–740.

Horton N, Lewis M. 1992. Calculation of the free energy of association for protein complexes. *Protein Sci 1*:169–181.

Ito W, Yasui H, Kurosawa Y. 1995. Mutations in the complementarity-determining regions do not cause differences in free energy during the process of for-

mation of the activated complex between an antibody and the corresponding protein antigen. *J Mol Biol 248*:729–732.
Janin J. 1995. Elusive affinities. *Proteins Struct Funct Genet 21*:30–39.
Janin J. 1997. The kinetics of protein–protein recognition. *Proteins Struct Funct Genet 28*:153–161.
Janin J, Chothia C. 1990. The structure of protein–protein recognition sites. *J Biol Chem 265*:16027–16030.
Jencks WP. 1981. On the attribution and additivity of binding-energies. *Proc Natl Acad Sci USA 78*:4046–4050.
Jin L, Wells JA. 1994. Dissecting the energetics of an antibody-antigen interface by alanine shaving and molecular grafting. *Protein Sci 3*:2351–2357.
Julin DA, Kirsch JF. 1989. Kinetic isotope effect studies on aspartate aminotransferase: Evidence for a concerted 1,3 prototropic shift mechanism for the cytoplasmic isozyme and L-aspartate and dichotomy in mechanism. *Biochemistry 28*:3825–3833.
Kam-Morgan LNW, Smith-Gill SJ, Taylor MG, Zhang L, Wilson AC, Kirsch JK. 1993. High-resolution mapping of the HyHEL-10 epitope of chicken lysozyme by site-directed mutagenesis. *Proc Natl Acad Sci USA 90*:3958–3962.
Kozack RE, Subramanian S. 1993. Brownian dynamics simulations of molecular recognition in an antibody-antigen system. *Protein Sci 2*:915–926.
Malcolm BA, Rosenberg S, Corey MJ, Allen JS, deBaetselier A, Kirsch JF. 1989. Site-directed mutagenesis of the catalytic residues Asp-52 and Glu-35 of chicken egg white lysozyme. *Proc Natl Acad Sci USA 86*:133–137.
Matouschek A, Serrano L, Fersht AR. 1992. The folding of an enzyme. IV. Structure of an intermediate in the refolding of barnase analysed by a protein engineering procedure. *J Mol Biol 224*:819–835.
Matsumura I, Kirsch JF. 1996. Is aspartate 52 essential for catalysis by chicken egg white lysozyme? The role of natural substrate-assisted hydrolysis. *Biochemistry 35*:1881–1889.
Nieba L, Krebber A, Plückthun A. 1996. Competition BIAcore for measuring true affinities: Large differences from values determined from binding kinetics. *Anal Biochem 234*:155–165.
Padlan EA, Silverton EW, Sheriff S, Cohen GH, Smith-Gill SJ, Davies DR. 1989. Structure of an antibody–antigen complex: Crystal structure of the HyHEL-10 Fab-lysozyme complex. *Proc Natl Acad Sci USA 86*:5938–5942.
Rajpal A, Taylor MG, Kirsch JF. 1998. Qualitative evaluation of the complete chicken lysozyme epitope in the HyHEL-10 Fab complex: Free energies and kinetics. *Protein Sci 7*:1868–1874.
Raman CS, Jemmerson R, Nall BT, Allen MJ. 1992. Diffusion-limited rates for monoclonal antibody binding to cytochrome *c*. *Biochemistry 31*:10370–10379.
Ray AA. 1982. *SAS User's guide: Basics, 1982 edition*. Cary, North Carolina: SAS Institute.
Richards FM. 1974. The interpretation of protein structures: Total volume, group volume distributions and packing density. *J Mol Biol 82*:1–14.
Sadana A, Chen Z. 1996. Influence of non-specific binding on antigen-antibody binding kinetics for biosensor applications. *Biosens Bioelectron 11*:17–33.
Sancho J, Fersht AR. 1992. Dissection of an enzyme by protein engineering: The N and C-terminal fragments of barnase form a native-like complex with restored enzymic activity. *J Mol Biol 224*:741–747.
Sancho J, Meiering EM, Fersht AR. 1991. Mapping transition states of protein unfolding by protein engineering of ligand-binding sites. *J Mol Biol 221*:1007–1014.
Schreiber G, Fersht AR. 1995. Energetics of protein–protein interactions: Analysis of the barnase–barstar interface by single mutations and double mutant cycles. *J Mol Biol 248*:478–486.
Schuck P, Minton AP. 1996. Kinetic analysis of biosensor data: Elementary tests for self-consistency. *Trends Biochem Sci 21*:458–460.
Serrano L, Kellis JT Jr, Cann P, Matouschek A, Fersht AR. 1992a. The folding of an enzyme. II. Substructure of barnase and the contribution of different interactions to protein stability. *J Mol Biol 224*:783–804.
Serrano L, Matouschek A, Fersht AR. 1992b. The folding of an enzyme. III. Structure of the transition state for unfolding of barnase analysed by a protein engineering procedure. *J Mol Biol 224*:805–818.
Serrano L, Matouschek A, Fersht AR. 1992c. The folding of an enzyme. VI. The folding pathway of barnase: Comparison with theoretical models. *J Mol Biol 224*:847–859.
Shih P, Malcolm BA, Rosenberg S, Kirsch JF, Wilson AC. 1993. Reconstruction and testing of ancestral proteins. *Methods Enzymol 224*:576–590.
Shugar D. 1952. The measurement of lysozyme activity and the ultra-violet inactivation of lysozyme. *Biochim Biophys Acta 8*:302–309.
Solc K, Stockmayer WH. 1973. Kinetics of diffusion-controlled reaction between chemically asymmetric molecules. II. Approximate steady-state solution. *Int J Chem Kinet 5*:733–752.
Sophianopoulos AJ, Rhodes CK, Holcomb DN, Van Holde KE. 1962. Physical studies of lysozyme. I. Characterization. *J Biol Chem 237*:1107–1112.
Tsai CJ, Xu D, Nussinov R. 1997. Structural motifs at protein–protein interfaces: Protein cores versus two-state and three-state model complexes. *Protein Sci 6*:1793–1805.
Tsumoto K, Ogasahara K, Ueda Y, Watanabe K, Yutani K, Kamagai I. 1995. Role of tyr residues in the contact region of anti-lysozyme monoclonal antibody HyHEL-10 for antigen binding. *J Biol Chem 270*:18551–18557.
Tsumoto K, Ogasahara K, Ueda Y, Watanabe K, Yutani K, Kamagai I. 1996. Role of salt bridge formation in antigen–antibody interaction. *J Biol Chem 271*:32612–32616.
Van Oss CJ. 1995. Hydrophobic, hydrophilic and other interactions in epitope-paratope binding. *Mol Immunol 32*:199–211.
Wells JA. 1991. Systematic mutational analyses of protein–protein interfaces. *Methods Enzymol 202*:390–411.
Williams DC Jr, Benjamin DC, Poljak RJ, Rule GS. 1996. Global changes in amide hydrogen exchange rates for a protein antigen in complex with three different antibodies. *J Mol Biol 257*:866–876.